Optimum Mixed-State Discrimination for Noisy Entanglement-Enhanced Sensing

Quntao Zhuang,[1,2,*] Zheshen Zhang,[1] and Jeffrey H. Shapiro[1]

[1]*Research Laboratory of Electronics, Massachusetts Institute of Technology, Cambridge, Massachusetts 02139, USA*
[2]*Department of Physics, Massachusetts Institute of Technology, Cambridge, Massachusetts 02139, USA*

Quantum metrology utilizes nonclassical resources, such as entanglement or squeezed light, to realize sensors whose performance exceeds that afforded by classical-state systems. Environmental loss and noise, however, easily destroy nonclassical resources and, thus, nullify the performance advantages of most quantum-enhanced sensors. Quantum illumination (QI) is different. It is a robust entanglement-enhanced sensing scheme whose 6 dB performance advantage over a coherent-state sensor of the same average transmitted photon number survives the initial entanglement's eradication by loss and noise. Unfortunately, an implementation of the optimum quantum receiver that would reap QI's full performance advantage has remained elusive, owing to its having to deal with a huge number of very noisy optical modes. We show how sum-frequency generation (SFG) can be fruitfully applied to optimum multimode Gaussian-mixed-state discrimination. Applied to QI, our analysis and numerical evaluations demonstrate that our SFG receiver saturates QI's quantum Chernoff bound. Moreover, augmenting our SFG receiver with a feedforward (FF) mechanism pushes its performance to the Helstrom bound in the limit of low signal brightness. The FF-SFG receiver, thus, opens the door to optimum quantum-enhanced imaging, radar detection, state and channel tomography, and communication in practical Gaussian-state situations.

Introduction.—Entanglement is essential for device-independent quantum cryptography [1], quantum computing [2], and quantum-enhanced metrology [3]. It has also been employed in frequency and phase estimation to beat their standard quantum limits on measurement precision [4–10]. Furthermore, entanglement has applications across diverse research areas, including dynamic biological measurement [11], delicate material probing [12], gravitational wave detection [13], and quantum lithography [14]. Entanglement, however, is fragile; it is easily destroyed by quantum decoherence arising from environmental loss and noise. Consequently, the entanglement-enabled performance advantages of most quantum-enhanced sensing schemes quickly dissipate with increasing quantum decoherence, challenging their merits for practical situations.

Quantum illumination (QI) is an entanglement-enhanced paradigm for target detection that thrives on entanglement-breaking loss and noise [15–22]. Its optimum quantum receiver enjoys a 6 dB advantage in error-probability exponent over optimum classical sensing using the same transmitted photon number. Remarkably, QI's advantage occurs despite the initial entanglement being completely destroyed.

To date, the only in-principle realization of QI's optimum quantum receiver requires a Schur transform on a quantum computer [23], so that its physical implementation is unlikely to occur in the near future. At present, the best known suboptimum QI receivers [20,21]—one of which, the optical parametric amplifier (OPA) receiver, has been

demonstrated experimentally [21]—can only realize a 3 dB error-probability exponent advantage. Bridging the 3 dB performance gap between the suboptimum and optimum receivers with an implementation more feasible than a quantum computer is of particular significance for its application potential and for its deepening our understanding of entanglement-enhanced metrology.

In this Letter, we present an optimum QI-receiver architecture based on sum-frequency generation (SFG). In the weak-signal limit, the SFG unitary maps QI target detection to the well-studied problem of single-mode coherent state discrimination (see Ref. [24] for a review). Analytical calculation and Monte Carlo simulations confirm that this SFG receiver's performance approaches QI's quantum Chernoff bound (QCB) [18] asymptotically. Adding a feedforward (FF) mechanism yields the FF-SFG receiver, whose error probability achieves the Helstrom bound [33]. The FF-SFG receiver is potentially promising for other quantum-enhanced sensing scenarios, such as phase estimation, and it enlarges the toolbox for quantum-state discrimination [34–47]. In particular, it is the first architecture—short of a quantum computer—for optimum discrimination of multimode Gaussian mixed states, a major step beyond the optimum discrimination of single-mode pure states [48–51].

Target detection.—QI target detection works as follows [18]. An entanglement source generates $M \gg 1$ signal-idler mode pairs, having photon annihilation operators $\{\hat{c}_{S_{0_m}}, \hat{c}_{I_{0_m}} : 1 \leq m \leq M\}$, with each pair being in a two-mode squeezed-vacuum state of mean photon number

$2N_S \ll 1$. The signal modes probe for the presence of a weakly reflecting target embedded in a bright background, under the assumption that it is equally likely to be absent or present, while the idler modes are retained for subsequent joint measurement with light collected from the region interrogated by the signal modes. (We shall assume lossless idler storage, so that the idler modes used for that joint measurement satisfy $\hat{c}_{I_m} = \hat{c}_{I_{0_m}}$.) When the target is present (hypothesis $h = 1$), the returned signal modes are $\hat{c}_{S_m} = \sqrt{\kappa}\hat{c}_{S_{0_m}} + \sqrt{1-\kappa}\hat{c}_{N_m}$, where $\kappa \ll 1$ is the round-trip transmissivity and the $\{\hat{c}_{N_m}\}$ are noise modes in thermal states containing $N_B/(1-\kappa) \gg 1$ photons on average. When the target is absent (hypothesis $h = 0$), the returned signal modes are $\hat{c}_{S_m} = \hat{c}_{N_m}$, where the $\{\hat{c}_{N_m}\}$ are now taken to be in thermal states with average photon number N_B [52].

Omitting the $\kappa N_S \ll N_B$ contribution to $\langle\hat{c}_{S_m}^\dagger \hat{c}_{S_m}\rangle$ when the target is present, and conditioned on $h = j$, the $\{\hat{c}_{S_m}, \hat{c}_{I_m}\}$ constitute a set of independent, identically distributed (iid) mode pairs that are in zero-mean Gaussian states with a Wigner covariance matrix

$$\Lambda_j = \frac{1}{4}\begin{pmatrix} (2N_B+1)\mathbf{I} & 2C_p\mathbf{Z}\delta_{1j} \\ 2C_p\mathbf{Z}\delta_{1j} & (2N_S+1)\mathbf{I} \end{pmatrix}, \qquad (1)$$

where $\mathbf{I} = \mathrm{diag}(1,1)$, $\mathbf{Z} = \mathrm{diag}(1,-1)$, δ_{ij} is the Kronecker delta function, and $C_p = \sqrt{\kappa N_S(N_S+1)}$ is the phase-sensitive cross-correlation that exists when the target is present. The task of QI target detection is, thus, minimum error-probability discrimination between two M-mode-pair, zero-mean Gaussian states that are characterized by the $\{\Lambda_j\}$.

For equally likely hypotheses, the minimum error-probability quantum measurement for discriminating between states with density operators $\hat{\rho}_0$ and $\hat{\rho}_1$ is the Helstrom measurement $u(\hat{\rho}_1 - \hat{\rho}_0)$, where $u(x) = 1$ for $x \geq 0$ and 0, otherwise [33]. Absent the availability of a quantum computer, the best known QI receivers have error-probability exponents that are 3 dB inferior to optimum quantum reception. These suboptimum receivers use Gaussian local operations on each mode pair plus photon-number resolving measurements and, hence, belong to the class of local operations plus classical communication (LOCC). Their suboptimality follows because LOCC is not optimum for general mixed-state discrimination [53,54].

To go beyond LOCC, we will employ SFG. The QI transmitter uses a continuous-wave spontaneous parametric downconverter (SPDC) to generate $M \gg 1$ signal-idler mode pairs—at frequencies $\{\omega_{S_m}, \omega_{I_m}\}$—during target-region interrogation. These mode pairs originate from a single-mode pump $\hat{b}$ at frequency $\omega_b = \omega_{S_m} + \omega_{I_m}$. Each mode has average photon number N_S and each mode pair has a phase-sensitive cross-correlation $\sqrt{N_S(N_S+1)}$. SFG

is SPDC's inverse process: M independent signal-idler mode pairs with the same phase-sensitive cross-correlation can combine, coherently, to produce photons at the pump frequency. It is natural, therefore, to explore SFG in seeking an optimum QI receiver, because the phase-sensitive cross-correlation C_p in Eq. (1) is the signature of target presence. We begin with some foundational results for SFG.

Sum-frequency generation.—We will describe SFG by Schrödinger evolution for $t \geq 0$ under interaction Hamiltonian

$$\hat{H}_I = \hbar g \sum_{m=1}^{M}(\hat{b}^\dagger \hat{a}_{S_m}\hat{a}_{I_m} + \hat{b}\hat{a}_{S_m}^\dagger \hat{a}_{I_m}^\dagger), \qquad (2)$$

with $M \gg 1$, where $\hbar$ is the reduced Planck constant and g is the interaction strength. We will assume that at time $t = 0$ the $\{\hat{a}_{S_m}, \hat{a}_{I_m}\}$ mode pairs (at frequencies $\{\omega_{S_m}, \omega_{I_m}\}$) are in iid zero-mean Gaussian states, while the $\hat{b}$ sum-frequency mode (at frequency $\omega_b = \omega_{S_m} + \omega_{I_m}$) is in its vacuum state. We will assume that the state evolution stays wholly within the low-brightness, weak cross-correlation regime wherein $n_s(t) \equiv \langle\hat{a}_{S_m}^\dagger \hat{a}_{S_m}\rangle_t \ll 1$, $n_i(t) \equiv \langle\hat{a}_{I_m}^\dagger \hat{a}_{I_m}\rangle_t \ll 1$, and $|C(t)|^2 \equiv |\langle\hat{a}_{S_m}\hat{a}_{I_m}\rangle_t|^2 \ll n_s(t), n_i(t)$ for all time, where $\langle\cdot\rangle_t$ denotes averaging with respect to the state at time t. The qubit approximation to this evolution leads to the analytical results [24]

$$C(t) = C(0)\cos(\sqrt{M}gt), \qquad (3a)$$

$$b(t) = -i\sqrt{M}C(0)\sin(\sqrt{M}gt), \qquad (3b)$$

$$n_s(t) = n_s(0), \qquad n_i(t) = n_i(0), \qquad (3c)$$

$$n_b(t) = [M|C(0)|^2 + n_i(0)n_s(0)]\sin^2(\sqrt{M}gt), \qquad (3d)$$

where $b(t) \equiv \langle\hat{b}\rangle_t$ and $n_b(t) \equiv \langle\hat{b}^\dagger\hat{b}\rangle_t$. The average photon numbers in the $\{\hat{a}_{S_m}, \hat{a}_{I_m}\}$ are constant, in this approximation, because each mode's $n_b(t)/M$ contribution to the sum-frequency mode's average photon number is negligible. Equations (3) agree very well with numerical results for $M = 1, 2$, and 3 [24]. For any M they reveal a coherent oscillation between the $\hat{b}$ mode's mean field and the cross-correlation in all signal-idler mode pairs, plus an additional M-independent oscillation in the $\hat{b}$ mode's average photon number from the weak thermal-noise contribution [$\propto n_i(0)n_s(0)$], to $n_b(t)$.

Optimum receiver design.—Were $\langle\hat{c}_{S_m}^\dagger \hat{c}_{S_m}\rangle \ll 1$ under both hypotheses, QI's returned-signal and retained-idler mode pairs would satisfy the low-brightness conditions needed for Eqs. (3) to apply. Then, when these mode pairs undergo SFG with the sum-frequency mode $\hat{b}$ initially in its vacuum state, $\hat{b}$'s output state at $t = \pi/2\sqrt{M}g$ would be approximately a weak thermal state (average photon number $n_T = \langle\hat{c}_{I_m}^\dagger \hat{c}_{I_m}\rangle\langle\hat{c}_{S_m}^\dagger \hat{c}_{S_m}\rangle$) when $h = 0$, or a coherent state (with mean field $-i\sqrt{M}C_p$) embedded in a weak

thermal background (average photon number n_T) when $h = 1$. Minimum error-probability discrimination between the two hypotheses, based on $\hat{b}$'s output state, is then a single-mode Gaussian mixed-state problem [24]. Unfortunately, Eq. (1) implies that $\langle \hat{c}_{S_m}^{\dagger} \hat{c}_{S_m} \rangle_0 = N_B \gg 1$ under both hypotheses, violating the low-brightness condition. When these bright signal modes undergo SFG, they drive $\hat{b}$ to an equilibrium state [55], precluding the desired coherent conversion.

To resolve this $N_B \gg 1$ problem, we propose a receiver that uses K cycles of $\pi/2\sqrt{M}g$-duration SFG interactions, as shown in Fig. 1. With optimum choices of the $\{r_k, \varepsilon_k\}$, this figure represents the FF-SFG receiver; setting all the $\{r_k, \varepsilon_k\}$ to zero reduces it to the SFG receiver. We shall describe the FF-SFG receiver, but present performance results for both receivers. It suffices to consider a single cycle comprised of one SFG interaction, plus the pre-SFG signal slicing, the post-SFG signal combining, and the post-SFG photon-counting measurements.

Let $\{\hat{c}_{S_m}^{(k)}, \hat{c}_{I_m}^{(k)}\}$ be the signal-idler mode pairs at the input to the kth cycle for $0 \le k \le K-1$, with $\hat{c}_{S_m}^{(0)} = \hat{c}_{S_m}$ and $\hat{c}_{I_m}^{(0)} = \hat{c}_{I_m}$. A transmissivity $\eta \ll 1$ beam splitter taps a small portion of each $\hat{c}_{S_m}^{(k)}$ mode, yielding a low-brightness transmitted mode $\hat{c}_{S_m,1}^{(k)}$ to undergo a two-mode squeezing (TMS) operation $S(r_k)$ [56], with the $\hat{c}_{I_m}^{(k)}$ mode, and a high-brightness reflected mode $\hat{c}_{S_m,2}^{(k)}$ to be retained. For the FF-SFG receiver, the r_k value (which depends on $\tilde{h}_k = 0$ or 1, the minimum error-probability decision as to target absence
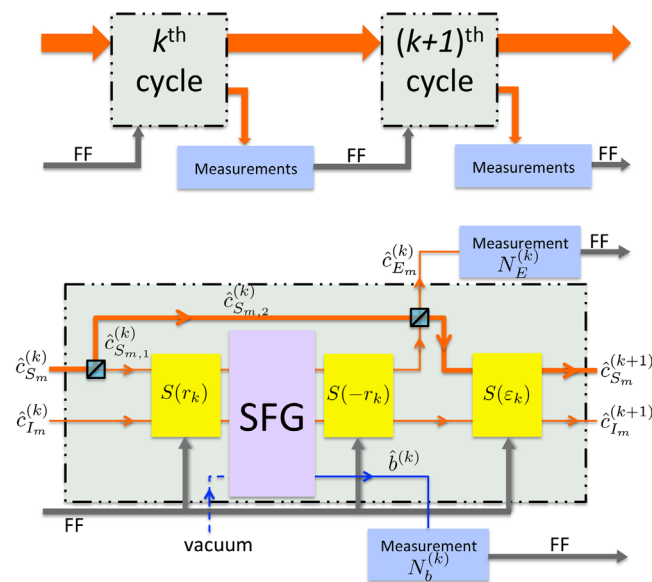

FIG. 1. Schematic of the FF-SFG receiver. Upper panel: two successive cycles. Lower panel: the components in the kth cycle. $S(\cdot)$: two-mode squeezing; SFG: sum-frequency generation; FF: feedforward operation.

or presence based on the measurement results from all prior cycles [58]) is chosen to almost purge any phase-sensitive cross-correlation between the $\{\hat{c}_{S_m,1}^{(k)}, \hat{c}_{I_m}^{(k)}\}$ mode pairs from the $S(r_k)$ operation's output mode pairs were $\tilde{h}_k$ a correct decision. Because $S(r_k)$'s output mode pairs are applied to a SFG process that converts any mode-pair phase-sensitive cross-correlation to a nonzero mean field for its sum-frequency ($\hat{b}^{(k)}$) mode's output, any significant mean field indicates that the $\tilde{h}_k$ decision was wrong. As shown in [24]: (1) $\hat{b}^{(k)}$ is not entangled with any other SFG output mode; and (2) each signal-idler mode pair emerging from SFG is in a Gaussian state. These facts allow us to use the weak TMS operation $S(\sqrt{\eta}C_{si}^{(k)} - r_k)$ to approximate the SFG operation on each signal-idler mode pair, where $C_{si}^{(k)} \equiv \langle \hat{c}_{S_m}^{(k)} \hat{c}_{I_m}^{(k)} \rangle$.

Following the kth cycle's SFG operation, we apply the TMS operation $S(-r_k)$ to each signal-idler mode pair. Under either hypothesis, the number of photons lost by the signal modes entering the SFG operation matches the number of photons gained by the $\hat{b}^{(k)}$ mode. The $S(-r_k)$ operation ensures that, when its signal-mode outputs are combined with the retained $\{\hat{c}_{S_m,2}^{(k)}\}$ modes on a second transmissivity-η beam splitter, the $\{\hat{c}_{E_m}^{(k)}\}$ output modes contain the same number of photons as the $\hat{b}^{(k)}$ mode. The photon-number measurements $\hat{b}^{(k)\dagger}\hat{b}^{(k)}$ and $\sum_{m=1}^{M} \hat{c}_{E_m}^{(k)\dagger} \hat{c}_{E_m}^{(k)}$ then provide outcomes $N_b^{(k)}$ and $N_E^{(k)}$ that are substantial when $\tilde{h}_k$ is incorrect, but negligible when $\tilde{h}_k$ is correct. These measurement outcomes are fed-forward for use in determining $\tilde{h}_{k+1}$, with $\tilde{h}_K$ being the receiver's final decision as to whether the target is absent or present.

The kth cycle is completed by a TMS operation $S(\varepsilon_k)$, with $\varepsilon_k = \sqrt{\eta}r_k$, that makes the phase-sensitive cross-correlation of the signal and idler inputs to the $(k+1)$th cycle independent of r_k. The first-order results for the conditional moments given $h = j$ are [24]

$$n_s^{(k)} \equiv \langle \hat{c}_{S_m}^{(k)\dagger} \hat{c}_{S_m}^{(k)} \rangle|_{h=j} = N_B, \quad (4a)$$

$$n_i^{(k)} \equiv \langle \hat{c}_{I_m}^{(k)\dagger} \hat{c}_{I_m}^{(k)} \rangle|_{h=j} = N_S, \quad (4b)$$

$$C_{si}^{(k)}|_{h=j} = jC_p[1 - \eta(1 + N_B)]^k. \quad (4c)$$

Feed-forward and decision.—All that remains to fully specify the FF-SFG receiver is to derive the optimum $\{r_k\}$ and $\{\tilde{h}_k\}$ values, and to choose an appropriate value for K, the number of cycles to be employed. To do so, we will draw on a connection to Dolinar's optimum receiver for binary coherent-state discrimination [49] by setting $r_k = 0$, to consider the SFG receiver, and omitting the small incoherent contribution to the $\hat{b}^{(k)\dagger}\hat{b}^{(k)}$ measurement.

Then, assuming $h = 1$, the kth cycle produces a $\hat{b}^{(k)}$ mode in a coherent state with average photon number $\langle N_b^{(k)} \rangle|_{h=1} = M\lambda_k^2$ and $\{\hat{c}_{E_m}^{(k)}\}$ modes in iid thermal states with total average photon number $\langle N_E^{(k)} \rangle|_{h=1} = M\lambda_k^2$, where $\lambda_k \equiv \sqrt{\eta} C_{si}^{(k)}|_{h=1}$. For η sufficiently small, the $h = 1$ statistics of $N^{(k)} \equiv N_b^{(k)} + N_E^{(k)}$ will match the photon-number statistics of the coherent state $|\sqrt{2M}\lambda_k\rangle$. On the other hand, the $h = 0$ statistics of $N^{(k)}$ are those of the vacuum state, i.e., $N^{(k)} = 0$ with probability one. Optimum binary coherent-state discrimination [49,51] applied to our problem, then, gives $r_k = r_{\tilde{h}_k}^{(k)}$, where (see Ref. [24] for an intuitive explanation)

$$r_{\tilde{h}_k}^{(k)} = \frac{\lambda_k}{2}\left(1 - \frac{(-1)^{\tilde{h}_k}}{\sqrt{1 - \exp\left[-2M\left(\sum_{\ell=0}^{k}\lambda_\ell^2 - \lambda_k^2/2\right)\right]}}\right). \quad (5)$$

Here, $\tilde{h}_k$ is the j value that maximizes $P_{h=j}^{(k)}$ [58], where the prior probabilities for the kth cycle, $\{P_{h=j}^{(k)} : j = 0, 1\}$, are the posterior probabilities of the $(k-1)$th cycle that are obtained from the Bayesian update rule [51,59],

$$P_{h=j}^{(k)} = \frac{P_{h=j}^{(k-1)} P_{BE}(N_b^{(k-1)}, N_E^{(k-1)}; j, r_{\tilde{h}_{k-1}}^{(k-1)})}{\sum_{j=0}^{1} P_{h=j}^{(k-1)} P_{BE}(N_b^{(k-1)}, N_E^{(k-1)}; j, r_{\tilde{h}_{k-1}}^{(k-1)})}, \quad (6)$$

for $1 \leq k \leq K - 1$, where $P_{BE}(N_b^{(k-1)}, N_E^{(k-1)}; j, r_{\tilde{h}_{k-1}}^{(k-1)})$ is the conditional joint probability of getting counts $N_b^{(k-1)}$ and $N_E^{(k-1)}$ given that the true hypothesis is j and $r_{k-1} = r_{\tilde{h}_{k-1}}^{(k-1)}$. The $S(r_{k-1})$-SFG-$S(-r_{k-1})$ cascade in the $(k-1)$th cycle is designed to make the photon fluxes that generate $N_b^{(k-1)}$ and $N_E^{(k-1)}$ much higher if $\tilde{h}_{k-1} \neq h$ than if $\tilde{h}_{k-1} = h$. Thus, the update rule will flip $\tilde{h}_k$ to the other hypothesis if too many photons are counted in the $(k-1)$th cycle; otherwise, $\tilde{h}_k = \tilde{h}_{k-1}$ will prevail.

To determine how many cycles must be run, we reason as follows. Suppose that $h = 1$ and we continue to neglect the small incoherent contribution to the $\hat{b}^{(k)\dagger}\hat{b}^{(k)}$. We then have that $N_T^{(K)} \equiv \sum_{k=0}^{K-1} N^{(k)} = 2M\sum_{k=0}^{K-1}\lambda_k^2$ is the total average photon number of all the measurements made in the FF-SFG receiver's K cycles. To ensure that the receiver's final decision, $\tilde{h}_K$, as to whether the target is absent ($\tilde{h}_K = 0$) or present ($\tilde{h}_K = 1$) is optimum, two conditions should be satisfied: (1) η is small enough that the qubit approximations in [24] are valid; and (2) K is large enough that $N_T^{(K)}/N_T^{(\infty)} = 1 - \epsilon$, for some pre-chosen $0 < \epsilon \ll 1$.

Performance.—We begin our performance evaluations for the FF-SFG and SFG receivers with some asymptotic results [24]. For η sufficiently small, the coherent and incoherent (thermal-state) contributions to $N_T^{(K)}$ are

$N_{T_{\text{coh}}}^{(K)} \simeq (1 - \epsilon)M\kappa N_S/N_B$ and $N_{T_{\text{therm}}}^{(K)} \simeq -N_S \ln(\epsilon)/2$, and the number of cycles employed is $K \simeq -\ln(\epsilon)/2\eta N_B$. Equations (4), which underlie these expressions, are valid only when $N_S \ll 1$. So, to get asymptotic results, we let $N_S \to 0$, to drive $N_{T_{\text{therm}}}^{(K)}$ to zero, and we increase the source's mode number, M, to keep $N_{T_{\text{coh}}}^{(K)}$ constant. In this regime, QI target detection with the FF-SFG and SFG receivers becomes one of discriminating the coherent state $|\sqrt{N_{T_{\text{coh}}}^{(K)}}\rangle$ from the vacuum. Like the case for the Dolinar receiver [49], the FF-SFG receiver's error probability should then approach the Helstrom bound $P_H = [1 - \sqrt{1 - \exp(-N_{T_{\text{coh}}}^{(K)})}]/2$, and, like the case for the Kennedy receiver [48], the SFG receiver's error-probability exponent should approach $N_{T_{\text{coh}}}^{(K)}$, which, for $\epsilon \to 0$, is both the QCB for the preceding coherent-state discrimination problem and that for QI target detection.

To explore how closely the FF-SFG and SFG receivers' error probabilities approach their asymptotic behavior, we performed Monte Carlo simulations using $N_S = 10^{-4}$, $\kappa = 0.01$, $N_B = 20$, $\eta = 0.002$, and $K = 42$. These parameter values are consistent with the qubit approximation's validity. We used 10^5 (for $\log_{10} M < 7.8$) to 10^6 simulation runs (for $\log_{10} M \geq 7.8$) to obtain our error-probability estimates [24]. Figure 2(a) compares M-dependent simulation results for the error probabilities of the FF-SFG, SFG, and OPA receivers with those of the homodyne receiver for coherent-state discrimination and the Helstrom bound with $N_{T_{\text{coh}}}^{(K)} = M\kappa N_S/N_B$. At all M values shown, both proposed receivers outperform the OPA receiver, with FF-SFG reception's performance approaching P_H. More importantly, our receivers asymptotically saturate the QCB. Figure 2(b) shows Monte Carlo results comparing the
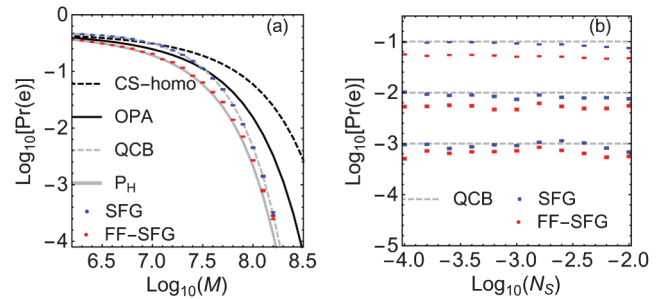
FIG. 2. (a) Error probabilities for the SFG, FF-SFG, and OPA receivers obtained from Monte Carlo simulations, plus analytical results for coherent-state (CS) discrimination with a homodyne receiver, and the Helstrom limit P_H when $N_{T_{\text{coh}}}^{(K)} = M\kappa N_S/N_B$. Parameter values are given in the text. (b) Error-probability exponents for the SFG and FF-SFG receivers versus source brightness, N_S, with M is chosen to keep the QI target-detection QCB at (top to bottom) 10^{-1}, 10^{-2}, or 10^{-3}. Simulations run were 10^6 for QCB = 10^{-3} and 10^5, otherwise.

error-probability exponents of the SFG and FF-SFG receivers with QI target-detection's QCB as a function of source brightness with M chosen to keep the QCB constant at 10^{-1}, 10^{-2}, or 10^{-3}. Increasing N_S increases $N_{T_{\mathrm{therm}}}^{(K)}$, so Fig. 2(b) shows that our receivers approach QCB performance over a wide range of noise values.

Discussion.—We have presented a structure for achieving asymptotically optimum performance in QI target detection. Compared to the Schur-transform approach to optimum mixed-state discrimination, the components of our FF-SFG and SFG receivers, albeit challenging, have simpler realizations. In particular, the required SFG can be implemented in an optical cavity or nonlinear waveguides [60], and its K cycles can be combined on a photonic integrated circuit [61–63]. Feed-forward operations have been successfully employed to obtain improved performance in the discrimination of coherent states [39–41], mixed states [64], and entangled states [65]. Furthermore, our receivers have other potential applications, including optimum reception for the QI communication protocol [66], and quantum state and channel tomography [67,68].

Three final points deserve mention. First, our receiver's slicing approach is analogous to that in [69], where it was shown that slicing could be used to achieve the Holevo capacity for classical information transmission over a pure-loss channel. Second, recent work [70] has shown that QI offers a great performance advantage in target detection in the Neyman-Pearson setting, when the miss probability, $\Pr(\tilde{h}_K \neq h | h = 1)$, is to be minimized subject to a constraint on the false-alarm probability, $\Pr(\tilde{h}_K \neq h | h = 0)$. The optimum quantum measurement for Neyman-Pearson detection, $u(\hat{\rho}_1 - \zeta\hat{\rho}_0)$ for an appropriately chosen real-valued ζ, is identical to that for minimum error-probability discrimination between $\hat{\rho}_1$ and $\hat{\rho}_0$ when $\zeta = \Pr(h = 0)/\Pr(h = 1)$. Thus, just as the Dolinar receiver can be initialized to achieve the Helstrom bound for coherent-state discrimination with unequal priors and, hence, for Neyman-Pearson discrimination, so too can our FF-SFG receiver for QI target detection. Finally, we note that the implementation burden on our FF-SFG receiver can be vastly reduced by replacing its feedforward stages with feedback stages; i.e., we implement only one cycle and feed back its optical outputs to its inputs while using its measurement outputs to adjust its r_k and ε_k values. Running this feedback arrangement through K cycles then yields the same output as the original feedforward setup but with only three squeezers, one SFG stage, and two beam splitters, instead of K times those numbers.

*quntao@mit.edu
[1] A. K. Ekert, Phys. Rev. Lett. **67**, 661 (1991).
[2] P. Shor, SIAM J. Comput. **26**, 1484 (1997).
[3] D. J. Wineland, J. J. Bollinger, W. M. Itano, F. L. Moore, and D. J. Heinzen, Phys. Rev. A **46**, R6797 (1992).
[4] J. P. Dowling, Phys. Rev. A **57**, 4736 (1998).
[5] I. Afek, O. Ambar, and Y. Silberberg, Science **328**, 879 (2010).
[6] G. Y. Xiang, B. L. Higgins, D. W. Berry, H. M. Wiseman, and G. J. Pryde, Nat. Photonics **5**, 43 (2011).
[7] T. Ono, R. Okamoto, and S. Takeuchi, Nat. Commun. **4**, 2426 (2013).
[8] P. M. Anisimov, G. M. Raterman, A. Chiruvelli, W. N. Plick, S. D. Huver, H. Lee, and J. P. Dowling, Phys. Rev. Lett. **104**, 103602 (2010).
[9] H. Yonezawa et al., Science **337**, 1514 (2012).
[10] L. Czekaj, A. Przysiezna, M. Horodecki, and P. Horodecki, Phys. Rev. A **92**, 062303 (2015).
[11] M. A. Taylor, J. Janousek, V. Daria, J. Knittel, B. Hage, H.-A. Bachor, and W. P. Bowen, Nat. Photonics **7**, 229 (2013).
[12] F. Wolfgramm, C. Vitelli, F. A. Beduini, N. Godbout, and M. W. Mitchell, Nat. Photonics **7**, 28 (2013).
[13] LIGO Scientific Collaboration, Nat. Phys. **7**, 962 (2011).
[14] M. D'Angelo, M. V. Chekhova, and Y. Shih, Phys. Rev. Lett. **87**, 013602 (2001).
[15] M. F. Sacchi, Phys. Rev. A **72**, 014305 (2005).
[16] M. F. Sacchi, Phys. Rev. A **71**, 062340 (2005).
[17] S. Lloyd, Science **321**, 1463 (2008).
[18] S.-H. Tan, B. I. Erkmen, V. Giovannetti, S. Guha, S. Lloyd, L. Maccone, S. Pirandola, and J. H. Shapiro, Phys. Rev. Lett. **101**, 253601 (2008).
[19] E. D. Lopaeva, I. R. Berchera, I. P. Degiovanni, S. Olivares, G. Brida, and M. Genovese, Phys. Rev. Lett. **110**, 153603 (2013).
[20] S. Guha and B. I. Erkmen, Phys. Rev. A **80**, 052310 (2009).
[21] Z. Zhang, S. Mouradian, F. N. C. Wong, and J. H. Shapiro, Phys. Rev. Lett. **114**, 110506 (2015).
[22] S. Barzanjeh, S. Guha, C. Weedbrook, D. Vitali, J. H. Shapiro, and S. Pirandola, Phys. Rev. Lett. **114**, 080503 (2015).
[23] D. Bacon, I. L. Chuang, and A. W. Harrow, Phys. Rev. Lett. **97**, 170502 (2006).
[24] See Supplemental Material at http://link.aps.org/supplemental/10.1103/PhysRevLett.118.040801 for derivations of results, a review of binary state discrimination, the intuition behind the FF-SFG receiver's Bayesian update rule, and a description of the Monte Carlo simulation procedure, which includes Refs. [25–32].
[25] K. M. R. Audenaert, J. Calsamiglia, R. Muńoz-Tapia, E. Bagan, L. Masanes, A. Acín, and F. Verstraete, Phys. Rev. Lett. **98**, 160501 (2007).
[26] S. Pirandola and S. Lloyd, Phys. Rev. A **78**, 012331 (2008).
[27] J. H. Shapiro, IEEE Trans. Inf. Theory **26**, 490 (1980).
[28] M. Takeoka and M. Sasaki, Phys. Rev. A **78**, 022320 (2008).
[29] C. Wittmann, M. Takeoka, K. N. Cassemiro, M. Sasaki, G. Leuchs, and U. L. Andersen, Phys. Rev. Lett. **101**, 210501 (2008).
[30] S. Pirandola, Phys. Rev. Lett. **106**, 090504 (2011).

[31] J. H. Shapiro, IEEE J. Sel. Top. Quantum Electron. **15**, 1547 (2009).

[32] R. M. Gagliardi and S. Karp, *Optical Communications* (Wiley, New York, 1976), p. 68.

[33] C. W. Helstrom, J. Stat. Phys. **1**, 231 (1969).

[34] A. Chefles, Contemp. Phys. **41**, 401 (2000).

[35] S. M. Barnett and S. Croke, Adv. Opt. Photonics **1**, 238 (2009).

[36] A. Chefles and S. M. Barnett, J. Mod. Opt. **45**, 1295 (1998).

[37] E. Andersson, S. M. Barnett, C. R. Gilson, and K. Hunter, Phys. Rev. A **65**, 052308 (2002).

[38] A. Chefles and S. M. Barnett, J. Phys. A **31**, 10097 (1998).

[39] J. Chen, J. L. Habif, Z. Dutton, R. Lazarus, and S. Guha, Nat. Photonics **6**, 374 (2012).

[40] F. E. Becerra, J. Fan, G. Baumgartner, J. Goldhar, J. T. Kosloski, and A. Migdall, Nat. Photonics **7**, 147 (2013).

[41] F. E. Becerra, J. Fan, and A. Migdall, Nat. Photonics **9**, 48 (2015).

[42] P. J. Mosley, S. Croke, I. A. Walmsley, and S. M. Barnett, Phys. Rev. Lett. **97**, 193601 (2006).

[43] R. B. M. Clarke, A. Chefles, S. M. Barnett, and E. Riis, Phys. Rev. A **63**, 040305 (2001).

[44] K. Tsujino, D. Fukuda, G. Fujii, S. Inoue, M. Fujiwara, M. Takeoka, and M. Sasaki, Phys. Rev. Lett. **106**, 250503 (2011).

[45] M. Takeoka, M. Sasaki, and N. Lütkenhaus, Phys. Rev. Lett. **97**, 040502 (2006).

[46] M. Takeoka, M. Sasaki, P. van Loock, and N. Lütkenhaus, Phys. Rev. A **71**, 022318 (2005).

[47] R. Nair, S. Guha, and S.-H. Tan, Phys. Rev. A **89**, 032318 (2014).

[48] R. S. Kennedy, Research Laboratory of Electronics, MIT, Quarterly Progress Report No. 108, pp. 219–225, 1973 (unpublished).

[49] S. J. Dolinar, Research Laboratory of Electronics, MIT, Quarterly Progress Report No. 111, pp. 115–120, 1973 (unpublished).

[50] M. Sasaki and O. Hirota, Phys. Rev. A **54**, 2728 (1996).

[51] A. Acín, E. Bagan, M. Baig, Ll. Masanes, and R. Muñoz-Tapia, Phys. Rev. A **71**, 032338 (2005).

[52] Changing $\langle \hat{c}_{N_m}^\dagger \hat{c}_{N_m} \rangle$ in this hypothesis-dependent manner is not physical, but, for $\kappa \ll 1$, the difference is small. We are following [18], where such a choice ensured that there was no passive signature to distinguish between $h = 0$ and $h = 1$, i.e., the sensor must actively illuminate the target region to make an informed decision.

[53] J. Calsamiglia, J. I. de Vicente, R. Muñoz-Tapia, and E. Bagan, Phys. Rev. Lett. **105**, 080504 (2010).

[54] S. Bandyopadhyay, Phys. Rev. Lett. **106**, 210402 (2011).

[55] R. Tanas, T. Gantsog, and R. Zawodny, Quantum Opt. **3**, 221 (1991).

[56] Here, we use $S(a)$ to denote the symplectic transform $S_2[\sinh^{-1}(a)]$ in the notation from [57].

[57] C. Weedbrook, S. Pirandola, R. García-Patrón, N. J. Cerf, T. C. Ralph, J. H. Shapiro, and S. Lloyd, Rev. Mod. Phys. **84**, 621 (2012).

[58] For h equally likely to be 0 or 1, we take $\tilde{h}_0$ to be 0 or 1 with equal probability.

[59] A. Assalini, N. Dalla Pozza, and G. Pierobon, Phys. Rev. A **84**, 022342 (2011).

[60] T. Guerreiro, E. Pomarico, B. Sanguinetti, N. Sangouard, J. S. Pelc, C. Langrock, M. M. Fejer, H. Zbinden, R. T. Thew, and N. Gisin, Nat. Commun. **4**, 2324 (2013).

[61] F. Najafi *et al.*, Nat. Commun. **6**, 5873 (2015).

[62] J. Mower, N. C. Harris, G. R. Steinbrecher, Y. Lahini, and D. Englund, Phys. Rev. A **92**, 032322 (2015).

[63] J. Carolan *et al.*, Science **349**, 711 (2015).

[64] B. L. Higgins, B. M. Booth, A. C. Doherty, S. D. Bartlett, H. M. Wiseman, and G. J. Pryde, Phys. Rev. Lett. **103**, 220503 (2009).

[65] Y. Lu, N. Coish, R. Kaltenbaek, D. R. Hamel, S. Croke, and K. J. Resch, Phys. Rev. A **82**, 042340 (2010).

[66] J. H. Shapiro, Phys. Rev. A **80**, 022320 (2009).

[67] A. I. Lvovsky and M. G. Raymer, Rev. Mod. Phys. **81**, 299 (2009).

[68] A. Acín, E. Jané, and G. Vidal, Phys. Rev. A **64**, 050302 (2001).

[69] M. P. da Silva, S. Guha, and Z. Dutton, Phys. Rev. A **87**, 052320 (2013).

[70] M. M. Wilde, M. Tomamichel, S. Lloyd, and M. Berta, arXiv:1608.06991.